Liquid and Ice Water and Glycerol/Water Glasses Compared by Infrared Spectroscopy from 295 to 12 K

Bogumil Zelent, Nathaniel V. Nucci, and Jane M. Vanderkooi*

Johnson Research Foundation, Department of Biochemistry and Biophysics, School of Medicine, University of Pennsylvania, Philadelphia, Pennsylvania 19104-6059

Received: June 6, 2004; In Final Form: September 13, 2004

Infrared absorption spectra for liquid and ice H_2O and D_2O and for protonated and deuterated glycerol/water glasses are compared in the spectral range of 1000−4000 cm^{-1} and the temperature range of 295−12 K. As temperature decreases, the absorbance bands of the OH and OD stretching modes of glycerol/water solution shift to lower frequency and the band intensifies and narrows. The center of the absorption band for OH stretch for glycerol/D_2O/H_2O solution (60/32/8 v/v) is at 3364 cm^{-1} at 295 K and at 3277 cm^{-1} at 25 K. The full width at half-maximum (fwhm) of the band is 259 cm^{-1} at 295 K and 186 cm^{-1} at 25 K. The width of the OH stretch band for D_2O that is doped with H_2O is 193 cm^{-1} in liquid (295 K) and 24 cm^{-1} in ice (12 K). The broader width for the OH stretch at 12 K for glycerol/water relative to that seen in ice is consistent with inhomogeneous broadening due to the glassy nature of glycerol/water solutions. The HOH and DOD bending (scissoring) bands for water in glycerol shift to higher frequency, and the band broadens as temperature decreases. In contrast, in water below the ice transition, the HOH bending band can no longer be seen. Glycerol C−H and C−D stretching and bending modes are temperature independent between 295 and 12 K. Absorption between 1350 and 1450 cm^{-1} was seen in glycerol when the hydroxyls are protonated, but not deuterated. This band is assigned to a bending motion involving the glycerol hydroxyl. Both ice and glycerol/water glass show temperature-dependent infrared changes, but for the glass shifts in bands are continuous and are consistent with an increase in the H-bonding strength with lowering temperature.

I. Introduction

Glycerol ($CH_2OHCHOHCH_2OH$) and water solutions are used in industry and the home for many applications, including antifreeze, detergents, cosmetics, and pharmaceutical products. Glycerol also serves in research as a biological cryoprotectant.[1] Biological macromolecules maintain structure in aqueous solutions of glycerol.[2] Glycerol and water solutions are optically clear over a wide range of temperatures, a property that make them useful for many spectroscopic studies of biomacromolecules over wide temperature excursions.

In this article, characteristics of glycerol/water solutions are examined by focusing on the contacts between water and the C−OH and C−H groups of glycerol over a temperature excursion of 295−12 K using infrared spectroscopy. The spectral features of the solution are contrasted with that of liquid water and ice. Large changes in the intensity, positions, and spectral bandwidths occur with hydrogen bonding. Groups involved in H-bonding are especially temperature dependent with stretching frequencies moving lower[3] and bending frequencies going higher as H-bonding strength increases with lowering temperature.[4,5] These temperature-dependent H-bonding changes have proven valuable in monitoring protein/solvent interactions by infrared (IR) spectroscopy.[6−8]

Figure 1 shows the structure of the molecules being studied, and the figure indicates some of their possible interactions; the figure is drawn to show that water and the C−OH group can be both H-bond donors and acceptors. Protonated and deuterated forms of glycerol and water were examined so all H's in the figure can be replaced by D's.

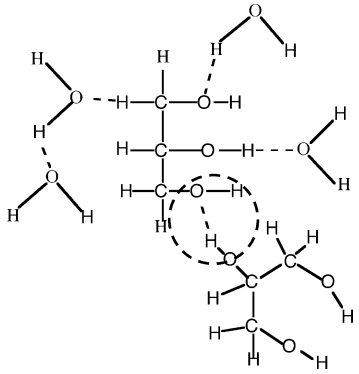

Figure 1. Scheme of some possible H-bonding interactions between water/glycerol, water/water, and glycerol/glycerol molecules. The circled group is discussed in the text.

The findings are that spectral changes in groups capable of H-bonding occur over the entire temperature range. The OH and OD stretches of glycerol and water go to lower frequency, and the HOH bending mode goes to higher frequency as temperature decreases from 295 to 12 K. The C−H and C−D stretching and bending frequencies are nearly temperature invariant over this range. H-bonding between glycerol molecules is also indicated by the spectra.

II. Materials and Methods

Materials. Water was deionized and then glass distilled. Glycerol (Sigma Grade), glycerol in which the hydroxyl groups

* To whom correspondence should be addressed. Phone 215-898-8783. E-mail: vanderko@mail.med.upenn.edu.

10.1021/jp0475584 CCC: $27.50
Published on Web 11/19/2004

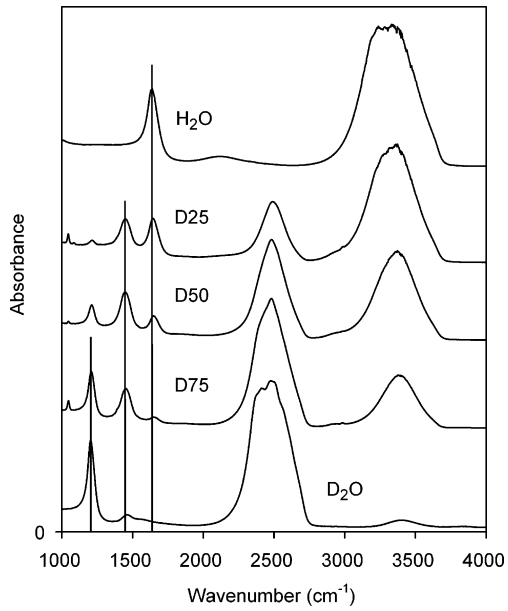

Figure 2. IR absorption spectra of HOH, DOH, and DOD. Top spectrum is for pure water; bottom spectrum is for commercial DOD. D25, D50, and D75 indicate 25, 50, and 75% of DOD added to HOH. Temperature: 20 °C. The spectra were taken in the ATR mode.

were deuterated (D_3-glycerol), and perdeuterated glycerol (D_8-glycerol) were obtained from Sigma/Aldrich Chemical Co. (St. Louis, MO). Deuterium oxide (99.9 atom % D) was obtained from Aldrich Chemical (Milwaukee, WI).

Spectroscopy. Infrared absorption spectra were obtained with a Bruker IFS 66 Fourier transform IR spectrophotometer (Bruker, Brookline, MA). The sample compartment was purged with nitrogen to reduce the contribution from water vapor, and light levels were monitored using an HgCdTe (MCT) detector. The spectral resolution was 2 cm^{-1}.

All spectra, except where indicated, were taken in the transmission mode. The temperature of the sample was maintained using an APD closed cycle Helitran cryostat (Advanced Research Systems, Allentown, PA). The spectra were obtained in sequence from high temperature to low temperature at 10° increments starting at 290 K, except for the lowest temperature, which was 12−20 K. The rate of cooling was about 1−2°/min. The temperature was measured with a silicon diode near the sample, and the temperature was controlled using a model 9650 temperature controller (Scientific Instruments, Palm Beach, FL). The outer cryostat windows were made of CaF_2. The inner cryostat windows, which experience the temperature gradient, were 2-mm thick and were made of ZnSe (Janos Technology, Inc., Townshend, VT). The solution was placed between two round CaF_2 plates (Janos Technology) with a 6-μm Teflon spacer.

Spectra of neat water, shown in Figure 2, were taken using the attenuated total reflectance (ATR) method. The ATR top plate was fitted with a 45° ZnSe 6 reflection crystal (Graseby Specac, Smyrna, GA).

The spectra were smoothed using a Savitsky-Golay smoothing algorithm. Widths and maximal positions of spectral bands were determined using PeakFit 4.11A (Systat, Inc., Richmond, CA).

III. Results

IR Spectra of HOH and DOD. The absorption of HOH, DOH, and DOD in the midrange infrared region using the ATR cell is documented in Figure 2. These spectra for water at 20 °C are well-known,[9,10] but they are included to serve as a reference for discussion of the following spectra. The OH and OD stretching regions are at 3400 and 2500 cm^{-1}. In neat DOD or HOH, the absorption includes both the symmetric and antisymmetric stretches.[11] In a mixture of DOD and HOH, the stretching modes become decoupled and the absorption arises from a simple stretching, but the width can be inhomogeneously broadened from various H-bonded forms of water. The OH stretching frequency is at 3386 cm^{-1} in the presence of 75% DOD, and the width is 279 cm^{-1}. The frequency maximum of OD in the presence of 75% HOH is 2495 cm^{-1}, and the width is 185 cm^{-1}.

TABLE 1: FTIR Absorption Spectra of D_2O/H_2O Using Attenuated Total Reflectance[a]

	HOH bend		HOD bend		DOD bend		O−H stretch		OD stretch	
	Pk	FW	Pk	FW	Pk	FW	Pk	FW	Pk	FW
H_2O	1647	92								
D_2O 25	1649	74	1449	75					2495	185
D_2O 50	1653	58	1449	86	1211	48			2484	225
D_2O 75	1657	59	1452	82	1209	52	3386	279		
D_2O					1206	56	3406	231		

[a] Data were fit by peak fit analysis. Pk-Peak center, cm^{-1}, of the peak with a Voigt fit. FW: fwhm, cm^{-1}.

A broad weak band centered at ~2130 cm^{-1} is evident in neat HOH. The corresponding band occurs at 1500 cm^{-1} for DOD. This band is attributed to the strong mixing of the overtone of a librational band with the bending mode fundamental.[12]

Focusing on the bending (scissoring) region, the bending frequency of HOH is at 1647 cm^{-1} and for DOD it is at 1206 cm^{-1} (Figure 2, top and bottom, respectively). The bending frequency of HOD is at 1449 cm^{-1}. There are several subtle details to be pointed out. First, the width of the bending mode absorption of DOD is the narrowest of the three water forms: its width is 56 cm^{-1} full width at half-maximum (fwhm). For HOD and HOH, the values are 82 and 92 cm^{-1}, respectively. Second, with increasing concentration of DOD, the peak position of the HOH bend absorption goes to higher frequency. To show this in the figure, a bar is placed at 1647 cm^{-1}. In pure water, the peak center position is at 1647 cm^{-1}; in 2:1 D_2O/H_2O, the position is at 1657 cm^{-1}. This is an indication of the coupling of vibrations from one molecule to the next. Details in the band shape and temperature dependence differences between −5 and 80 °C can be found in the article by Marechal.[13]

The peak positions and widths are summarized in Table 1. The extinction coefficients of the stretching and bending modes relative to each other are about the same as those found in the literature.[10,14,15]

IR Spectra of Ice as a Function of Temperature. Spectra of liquid water and ice taken in the transmission mode and transformed to absorption are shown in Figure 3. As reported in the literature,[12] as ice freezes the broad librational band at 2130 cm^{-1} in the liquid intensifies and shifts to 2230 cm^{-1}. The absorption band for the HOH bending mode is at 1647 cm^{-1} in liquid. With freezing, a broad band at 1557 cm^{-1} and a shoulder at 1500 cm^{-1} appear. Absorption in this region is attributed to a torsional overtone absorption, and the HOH bending mode absorption can no longer be seen.[12] As shown in Figure 3, the absorption at the lower part of this apparently double band increases, whereas the absorption at the higher frequency decreases with further lowering temperature. Absorption in the OH stretch region between 3000 and 3600 cm^{-1} is off-scale, but the band can be seen to shift to lower frequency

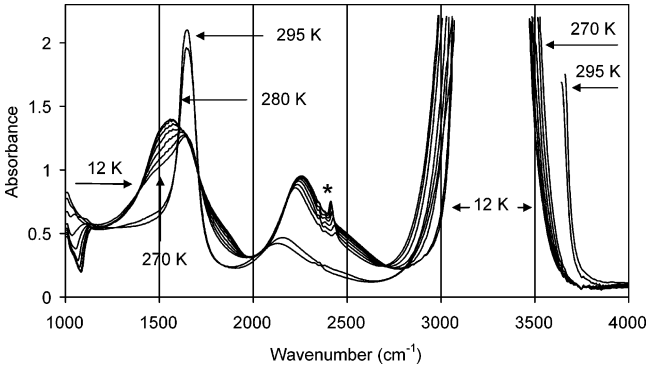

Figure 3. IR absorption spectra of liquid water and ice over a range of temperatures. Temperatures: 295, 280, 270, 210, 170, 130, 90, 50, and 12 K. The asterisk denotes a peak coming from contaminant D_2O.

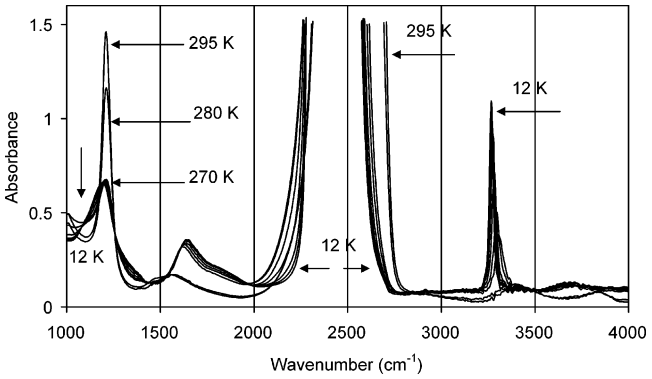

Figure 4. IR absorption spectra of D_2O doped with trace H_2O over a range of temperatures. Temperatures: 295, 280, 270, 230, 190, 150, 11, 70, 50 and 12 K.

at the freezing temperature (compare the spectra labeled 295 and 270 K). The OH band further narrows with temperature decrease.

Isotopic replacement for ice studies has proven useful for infrared and Raman studies because the H vibrations in D_2O glass are decoupled from the surroundings.[16,17] For us, isotope replacement has the further advantage that it allows the OH stretch region to be on-scale. Spectra of a D_2O sample that is doped with H_2O are shown in Figure 4. The OH stretch band maximum is ~3405 cm^{-1} at 295 K, but the H_2O is so dilute that the band is barely above the background. Upon freezing, the peak narrows and the OH stretch is seen in the spectrum as a sharp band that increases as temperature decreases.

The OH stretch region is seen in detail in Figure 5. With decreasing temperature, there is shifting and narrowing of the band. Values of position and width are given in Table 2.

The complementary experiment is to examine the OD stretch region in an H_2O sample that is doped with D_2O. In Figure 6, the OD stretch is examined in such a sample. For both OH and OD stretching bands, the width narrows and the frequency goes lower as temperature decreases.

The temperature dependence of the OD stretch region is seen in detail in Figure 7. The lowest temperatures are not shown, but fitted values for position and width are given in Table 2. The widths of the OH stretching band are 1.6 times the width of the OD stretching band comparable in the liquid, but this value is 3 times at 12 K. At low temperature, the width is likely to be significantly influenced by tunneling factors, which will be much larger for H.

IR Spectra of Solutions of HOH and DOD with Glycerol. We next demonstrate that the infrared absorption of HOH, DOD, and glycerol can be distinguished in solution and that spectral

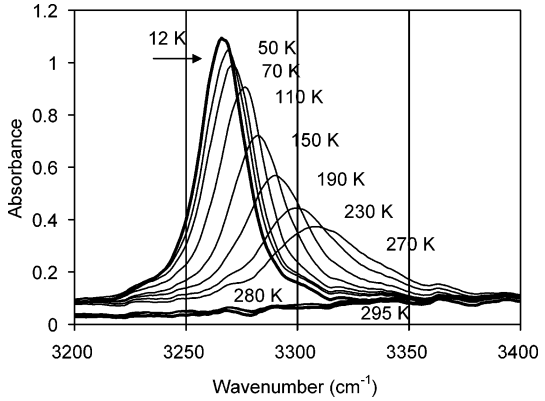

Figure 5. IR absorption spectra of the OH stretch region for H_2O doped in D_2O over a range of temperatures (from Figure 4). Temperatures indicated in the figure.

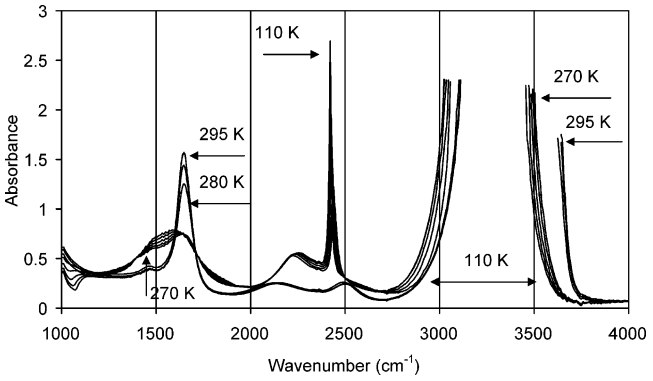

Figure 6. IR absorption spectrum of H_2O doped with ~2% D_2O over a range of temperatures. Other temperatures: 295, 290, 280, 270, 230, 190, 150, 110 K.

TABLE 2: Maximum of Absorption and Width, fwhm, of OH Stretching (in D_2O) and OD Stretching (in H_2O) Bands[a]

	OH		OD	
temp, K	ν_{max}, cm^{-1}	fwhm, cm^{-1}	ν_{max}, cm^{-1}	fwhm, cm^{-1}
295	3405	241	2508	148
280	3388	230	2497	146
270	3307	45	2442	30
210	3295	36	2434	21
150	3283	30	2425	14
110	3275	26	2421	10
70	3271	24	2417	8
12	3266	24	2415	8

[a] Data are peak fit analysis using Voigt fit of spectral bands shown in Figures 5 and 7.

features are recognizable both at high and low temperature. The IR spectrum of glycerol in the absence of water is shown in Figure 8A. Adding H_2O to glycerol results in a new absorbance at 1653 cm^{-1} (Figure 8B). The frequency of this peak due to HOH bending is higher relative to that observed in neat H_2O, which has the bending frequency at 1647 cm^{-1}, but is close to the peak position for HOH in DOD (Table 1). With D_2O present with glycerol, a new absorbance appeared at 2495 cm^{-1} (Figure 8C). This is identified as the OD stretching band, and its intensity increases and position shifts to 2429 cm^{-1} at low temperature. The absorbance in the HOD bending region, at ~1450 cm^{-1}, is also increased. The spectrum of D_3-glycerol is shown in Figure 8D. There is a sharp band at 1460 cm^{-1} and several smaller bands at lower frequency. We consider that the band at 1460 cm^{-1} is likely arising mainly of the CH_2 bending (scissoring) mode. Adding D_2O to D_3-glycerol results in a new

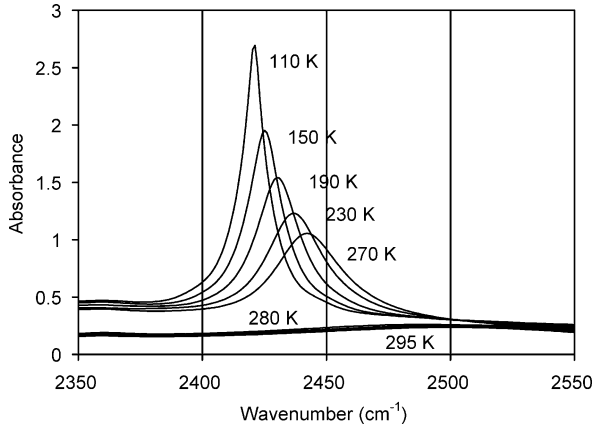

Figure 7. IR absorption spectrum of the OD stretch region for D_2O doped in H_2O at temperature indicated (from Figure 6).

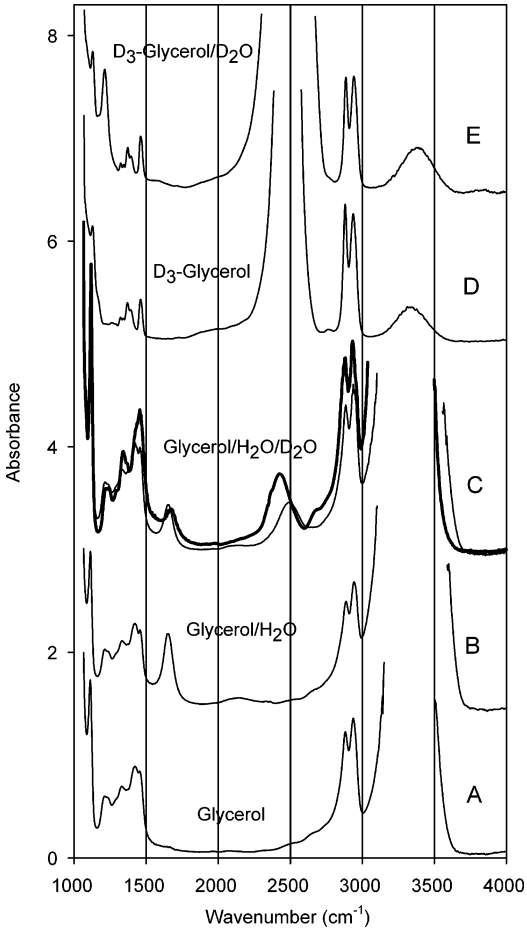

Figure 8. IR absorption spectra of glycerol with added H_2O and D_2O. (A) Neat glycerol. (B) 60% glycerol/40% H_2O (v/v). (C) 60% glycerol/32% H_2O/8% D_2O. (D) Neat D_3-glycerol. (E) 60% D_3-glycerol/40% D_2O. Temperature: 295 K, except for thick line at 20 K in spectrum C.

band at 1214 cm^{-1}. This is the DOD bending mode. Two bands at 2880−2885 and 2933−2940 cm^{-1} seen in Figure 8 are assigned to the symmetric and antisymmetric stretches of $-CH_2$.

Spectra of perdeuterated glycerol (D_8-glycerol) are shown in Figure 9. The bands of symmetric and antisymmetric $-CD_2$ stretches in D_8-glycerol are at 2105 and 2224 cm^{-1}. The spectrum of D_8-glycerol (Figure 9A) has a sharp peak at 1204 cm^{-1}; since this band is not seen in protonated glycerol (see Figure 8A), it likely arises from a CD_2 scissoring mode. Adding D_2O increased absorption in this region (Figure 5B) and the

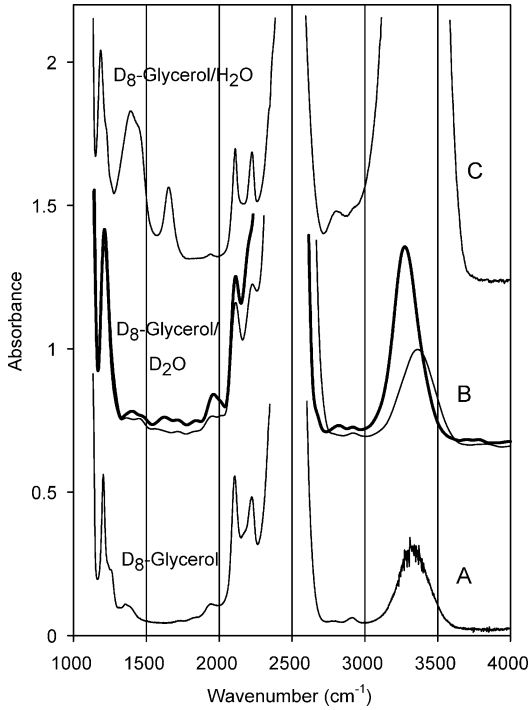

Figure 9. IR absorption spectra of D_8-glycerol with added H_2O and D_2O. (A) Neat D_8-glycerol. (B) 60% D_8-glycerol/40% D_2O (v/v). (C) 60% D_8-glycerol/40% H_2O. Temperature: 295 K, except for thick line at 12 K in spectrum B.

resultant band is broader than without D_2O. This result is consistent with its absorption being composed of contributions from both the DOD bending mode and the CD_2 bending mode.

The absorbance of the solution is not a simple sum of the components. In D_8-glycerol, there is very little absorption between 1400 and 1500 cm^{-1} (Figure 9B). When H_2O is added, as in Figure 9C, the HOH bending band is at 1657 cm^{-1}. A band also appears in the region around 1400−1450 cm^{-1} where HOD bend occurs. HOD absorbance is expected because the deuterons on glycerol hydroxyls are fully exchangeable. However, this band is clearly composed of at least two components.

To examine this feature, this region is expanded in Figure 10. With H_2O addition, a peak at 1657 cm^{-1} corresponding to the HOH bend appears, and this peak is shifted to higher frequency as temperature decreases. For 295 K, the fit parameters in cm^{-1} for the peaks of spectra of Figure 10 between 1300 and 1800 cm^{-1} were as follows: 1392 cm^{-1} (112), 1465 (62), 1657 (67). For 12 K, the fit parameters were as follows: 1413 (110), 1491 (59), 1677 (84). (The numbers in parentheses are the widths in cm^{-1}, fwhm.) Since 1465 and 1491 cm^{-1} are attributed to the HOD bend (Table 3), the new peaks are at 1392 and 1413 cm^{-1}. The lower frequency absorption may be coming from a bending mode of the group C−OH of glycerol that is H-bonded to another glycerol, as shown in Figure 1, indicated by a circle. This is also consistent with the difference in absorption between glycerol (Figure 8A) and D_3-glycerol (Figure 8D). In the case of glycerol, absorption in this range is discerned below the sharp absorbance bands that are also seen in D_3-glycerol.

Region between 1150 and 1800 cm^{-1}: Temperature Dependence of Glycerol Absorption and HOH Bending Modes. Absorption spectra of neat glycerol at temperatures from 270 to 12 K are shown in Figure 11. Very little absorption is seen in the region between 1550 and 1800 cm^{-1}, whereas in the region from 1150 to 1550 cm^{-1}, some peaks increase and others stay the same with lowering temperature. Spectra of 60/

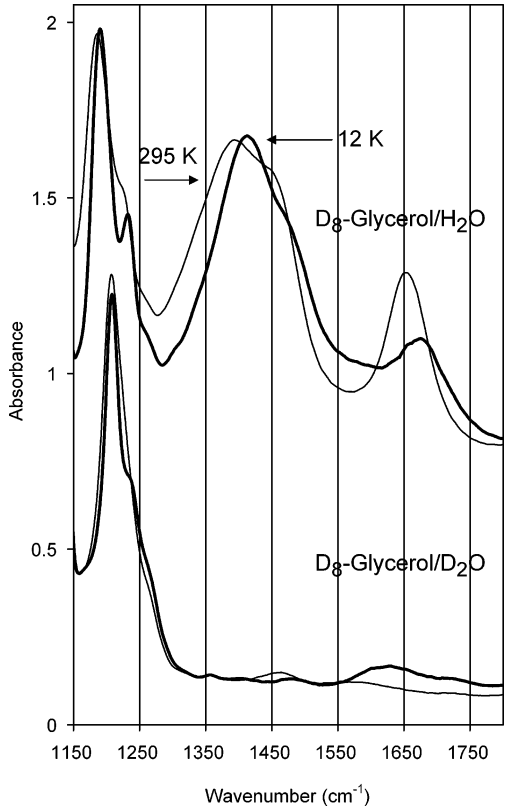

Figure 10. IR absorption spectra of D_8-glycerol/H_2O 60/40, v/v (top); D_8-glycerol/D_2O 60/40, v/v (bottom). Thin line: 295 K; thick line: 12 K.

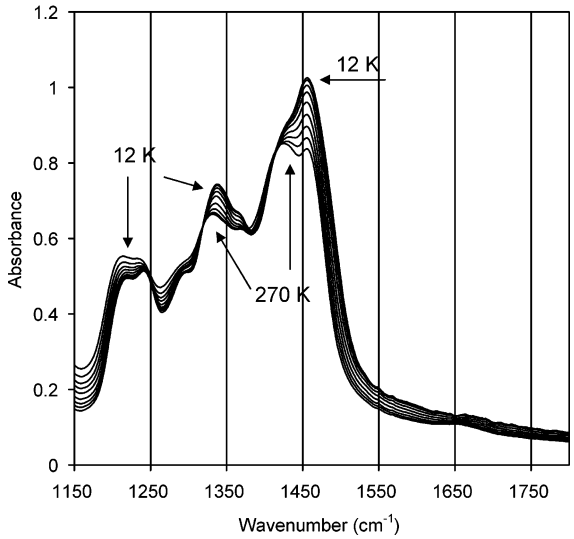

Figure 11. IR absorption spectra of glycerol. No water added. Spectra taken at 12, 70, 110, 150, 190, 210, 230, 250, and 270 K are shown.

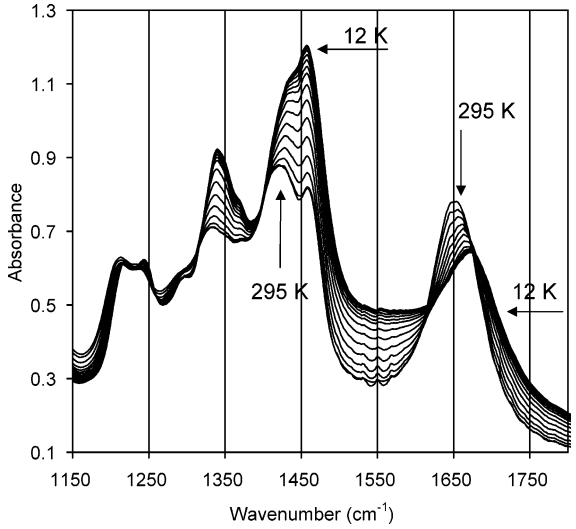

Figure 12. IR absorption spectra of glycerol and water (60/40, v/v). Temperatures at 295 and 12 K are indicated. Other temperatures were 290 to 30 K in 20° increments.

40 v/v glycerol/water are shown in Figure 12. In 60/40 v/v glycerol/water, the stoichiometry of OH for glycerol to the O on water is ∼1:1. The band position for the HOH bend is at 1653 cm^{-1} at 295 K. It goes to 1675 cm^{-1} at 12 K. The bandwidth increases, and the absorption decreases as temperature decreases.

For 40/60 v/v glycerol/water (Figure 13), the ratio of OH on glycerol to the O of water is ∼1:2. As expected for this solution, the absorption at 1652 cm^{-1} was relatively twice as high as seen in the 60/40 v/v glycerol/water (Figure 12). As temperature decreased, the ∼1652 cm^{-1} band shifted to higher frequency, but at around 210 K, the spectra began to show icelike features and no longer shifted higher (these spectra are not shown). The peak position of the HOH bending mode absorption at 230 K was 1662 cm^{-1} for both samples.

In Figures 11−12, positions at ∼1320 cm^{-1} and ∼1400 cm^{-1} appear to be invariant with temperature; they are, or closely approximate, isosbestic points. The band due to the HOH bend at ∼1650 cm^{-1} is shown on expanded scale in Figure 14. The position at 1680 cm^{-1} appears to approximate an isobestic point, but it is clear that at ∼1620 cm^{-1} there is no isosbestic. Continuous change in temperature is characteristic of a glass.

TABLE 3: Maximum of the Bending Absorption Bands (cm^{-1}) of HOH and DOD Mixed with Glycerols[a]

	temp, K	HOH bend	HOD bend	DOD bend	OH stretch	OD stretch
glycerol/H_2O (6/4)	295	1653 (73)				
	230	1662 (77)				
	12	1675 (77)				
glycerol/H_2O (4/6)	295	1652 (78)				
	230	1662 (82)				
D_2-glycerol/D_2O (6/4)	295	1657 (67)	1465 (62)			
	12	1677 (84)	1491 (59)			
glycerol/D_2O (6/4)	295			1213 (30)		
	12			1222 (26)		
D_3-glycerol/D_2O	295			1214 (39)		
	12			1225 (38)		
D_8-glycerol/D_2O/H_2O (60/32/trace)	295				3364 (259)	
	25				3277 (186)	
glycerol/H_2O/D_2O (60/32/8)	295					2495 (182)
	20					2429 (158)

[a] Pk-Peak center, cm^{-1}, of the peak with a Voigt fit. In parentheses: fwhm, cm^{-1}.

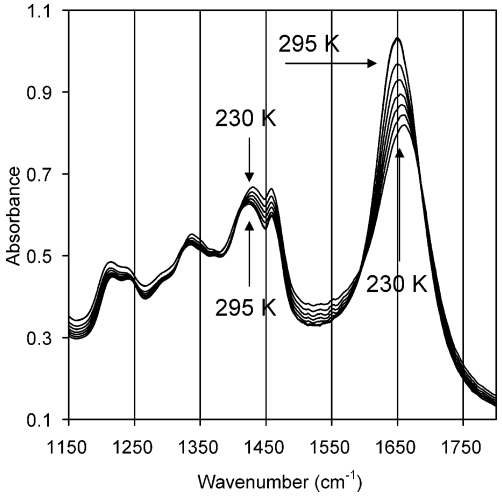

Figure 13. IR absorption spectra of glycerol and water (40/60, v/v). Temperatures at 295 and 230 K are indicated. Other temperatures were 290 to 230 K in 10° increments.

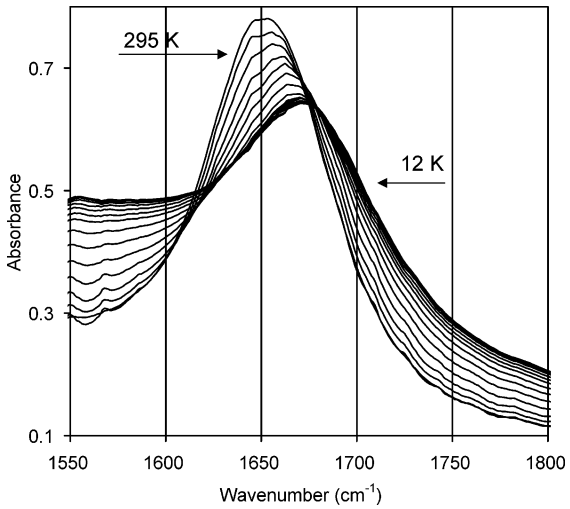

Figure 14. IR absorption spectra of glycerol and water (60/40, v/v). Details given in Figure 12.

Peak positions and bandwidths for bending modes of HOH in glycerol are summarized in Table 3.

Spectral Region of 1150−1550 cm^{-1} for DOD in D_3-Glycerol. The absorbance of DOD can also be specifically seen in glycerol. In Figure 15, absorbance spectra for D_3-glycerol are shown over the 295−12 K temperature range. In Figure 16, the spectra are shown for D_3-glycerol/D_2O 60/40 v/v. The arrow shows the absorbance of the bending mode of DOD. Like HOH, it shifts to higher frequency as temperature decreases.

Peak positions and bandwidths for bending modes of DOD in glycerol are also given in Table 3.

OH and OD Stretching Frequencies as a Function of Temperature. For all samples, the OH and OD stretching band is the strongest and, under conditions of our experiment, its absorption is off-scale when the respective isotopes of water and glycerol are used (seen in Figures 8 and 9). As for the ice studies, an on-scale OH stretching band is seen in a deuterated sample that includes a small amount of H_2O, and an on-scale OD stretching band is seen in a protonated sample containing a small amount of D_2O as is shown in Figure 8C,E. In neat H_2O or D_2O, the stretching mode band is composed of symmetric and anti-symmetric stretching mode contributions. In HOD the stretching modes are decoupled, and the absorption

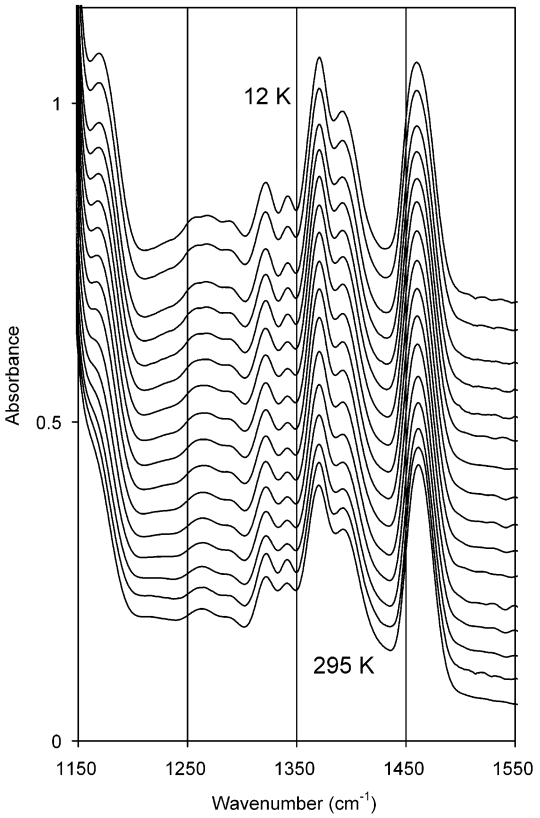

Figure 15. IR absorption spectra of D_3-glycerol. No water added. Temperature from bottom to top: 295, 290, 270, 250, 230, 210, 190, 170, 150, 130, 110, 90, 70, 50, 30, and 12 K.

is a simple stretching. The stretching absorption will also have contributions from glycerol. At 60/40 v/v glycerol/water, the group residue ratio is one O of glycerol per one O of water; therefore, the band should have about equal contribution from water and glycerol assuming approximately equal extinction coefficients.

The OH and OD stretch spectra at various temperatures are shown in Figures 17 and 18, respectively. As temperature is lowered, the OH and OD bands go to lower frequency and the bands narrow and intensify. The integrated area of the OH band increases by a factor of ∼1.5 in going from 300 to 25 K. As for the bending mode, the stretching bands do not show isosbestic points with temperature change. The amount of shift is consistent with the classification of a weak H-bond as given by Bratos and collaborators,[18] but the spectra remain broad, suggesting a distribution of H-bond strengths.

The instrumental spectral resolution was varied from 2 to 0.5 cm^{-1}. The absorption of the OH and OD bands shows no signs of resolution even at the lowest temperature even at the highest resolution (spectrum not shown). This is although there are chemically three kinds of hydroxyls; one from water and two from glycerol. The inhomogeneity of the OH and OD absorption bands is also contrasted with the narrow band seen in the ice.

Temperature Dependence of Water Bending and Stretching Bands. The peak positions in wavenumbers for HOH and DOD bending absorbance are plotted over the entire temperature range in Figure 19. The OH and OD stretching modes peak positions are presented in Figure 20. These figures reveal that the temperature dependencies of absorption of groups involved in H-bonding resemble each other. Note the difference in the *y*-axis: the spectral shifts with changing temperature are larger

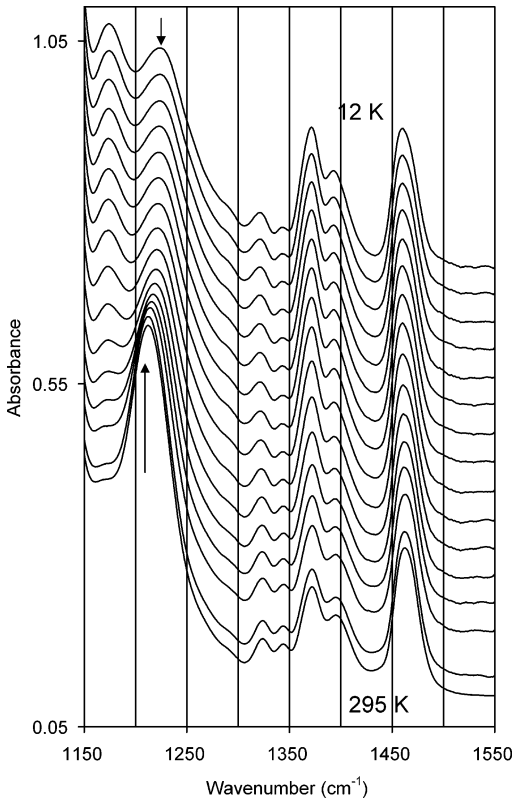

Figure 16. IR absorption spectra of D_3-glycerol/D_2O (60/40, v/v). Temperature from bottom to top: 295, 290, 270, 250, 230, 210, 190, 170, 150, 130, 110, 90, 70, 50, 30, and 12 K. Arrow indicates band attributed to the DOD bending mode.

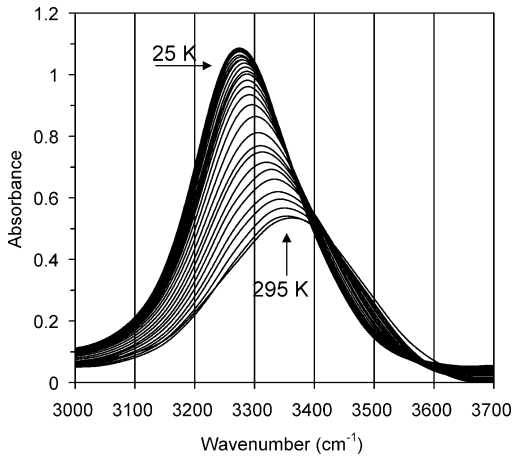

Figure 17. IR absorption spectra of the OH stretch region for D_8-glycerol/D_2O (60/40%) and trace H_2O. Spectra taken at 295 and 25 K are indicated. Other temperatures: 290 to 30 K in 10° increments.

for the H isotope relative to D. The glass transition for glycerol/water is at around 185 K.[19] It is evident that there are changes in the glass at temperatures lower than the glass transition.

Temperature Dependence of Absorbance from C−H Stretching Modes. Bands from C−H stretches at ∼2880 cm^{-1} and C−D stretches at ∼2105 cm^{-1} are seen in Figures 8 and 9, respectively. By using deuterated or protonated glycerol, the OH and OD stretching bands can be isolated from the aliphatic stretch region. An example of their spectra at various temperatures is shown in Figure 21. In D_3-glycerol there was no change in frequency over the temperature interval of nearly 300°.

The band fit parameters are given in Table 4. A third peak was also seen which may be due to the CH or CD stretching

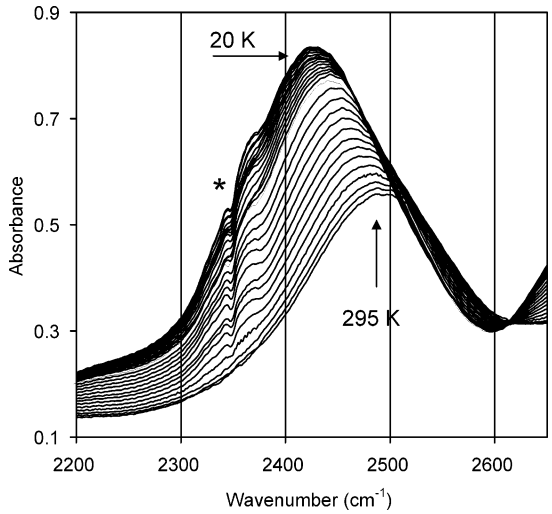

Figure 18. IR absorption of OD stretch region for 60% glycerol/32% H_2O/8% D_2O. Spectra taken at 295 and 20 K are indicated. Other temperatures: 290 to 30 K in 10° increments. Asterisk indicates absorption due to CO_2 in the optical path.

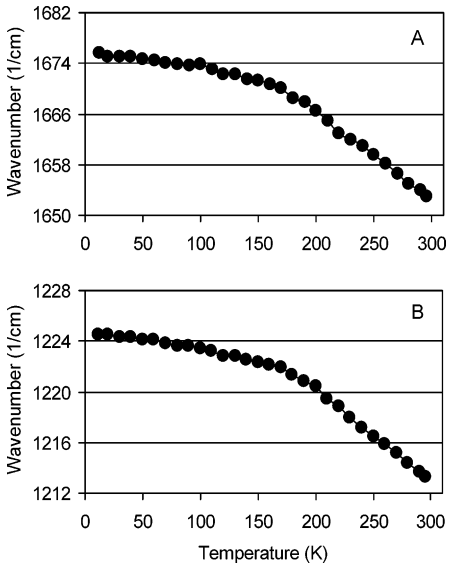

Figure 19. (A) HOH bend absorption maximum as a function of temperature. Conditions given in the legend of Figure 12. (B) DOD bend absorption maximum as a function of temperature. Conditions given in the legend of Figure 16.

from the central carbon of glycerol. For C−H, the third peak was at 2960 cm^{-1}, but its intensity was low, and thus it could not be reliably fit over the whole temperature range.

IV. Discussion

The goal of our work was to characterize glycerol/water solvent over the broad temperature range used for studying biological materials. The C−H and C−OH groups of glycerol have strong IR signatures. The C−OH group is also found in the amino acids serine and tyrosine, and C−OH is found in sugars, which are important in their own right and as components of DNA and RNA and many enzyme cofactors. C−H groups are found in all amino acids and in all other biological macromolecules. Therefore, the interaction of water with glycerol is informative for the general question of how water interacts with biological materials. Molecules that are classified as fragile glass formers lack strong intermolecular interactions; glycerol/water forms glasses of intermediate fragility.[20,21]

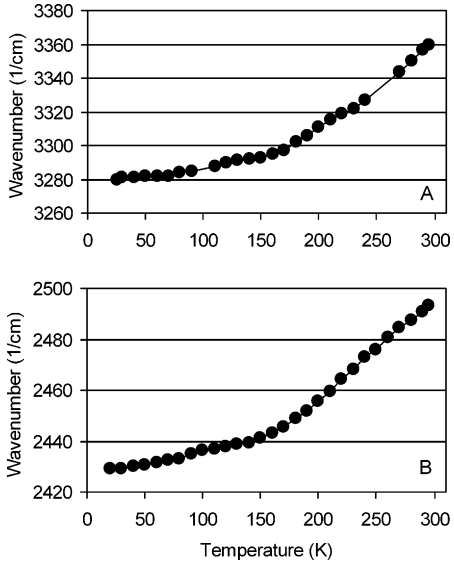

Figure 20. (A) OH stretch absorption maximum as a function of temperature. Conditions are given in the legend of Figure 17. (B) OD stretch absorption maximum as a function of temperature. Conditions are given in the legend of Figure 18.

Interactions within this solvent have received attention using many techniques.[22−26]

The results in this article contrast water in ice and water in glycerol/water solvent. Rearrangement of hydrogen positions at low temperature is well-known in ice, as pointed out by Pauling in 1935.[27] The zero-point entropy of ordinary ice (ice-Ih) is understood to result from disorder of possible hydrogen bonding connections.[28] The temperature dependence of the OH (in D_2O ice) and OD (in H_2O ice) stretching widths (Figures 19 and 20) suggests that a lower frequency mode, such as a phonon mode, may be coupled to its transition. We note also that KOH-doped ice-Ih is reported to show a transition at around 70 K,[29] which may be also playing a role here. The spectra that we present in this article give positions and line widths over a large temperature range. Their detailed interpretation will be a subject of further investigation.

The ice spectra are included to highlight differences in the water in ice and in glassy glycerol/water. In the liquid to ice transition for neat H_2O or D_2O, a sharp transition occurs and the bending mode becomes very weak, so that it is no longer seen (Figure 3). As stated by Hernandez et al., "It is reasonable to say that a bending mode band has never been observed for either pure H_2O or pure D_2O cubic or hexagonal ice."[30] In contrast, absorption of the bending mode for water in glycerol/water solution is seen even at the lowest temperature and

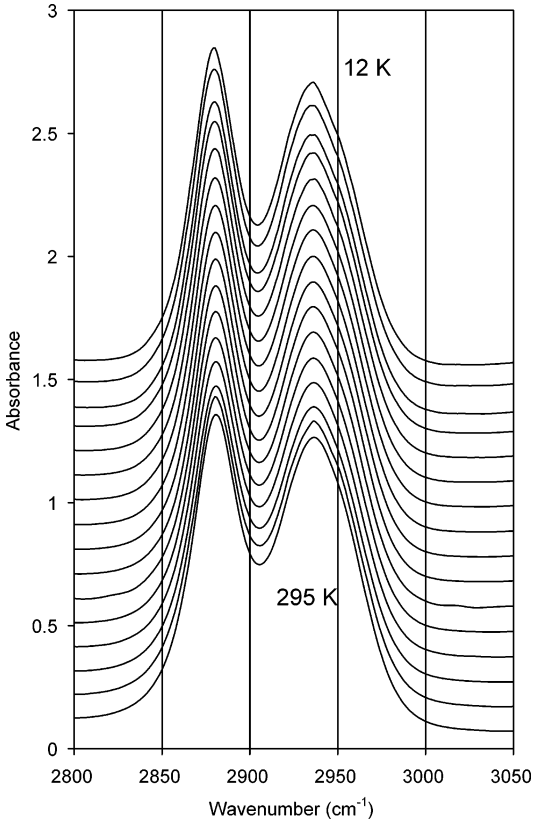

Figure 21. Symmetric and anti-symmetric CH stretching bands at various temperatures. D_3-glycerol, no added water. Temperatures from bottom are: 295, 290, 270, 250, 230, 210, 190, 170, 150, 130, 110, 90, 70, 50, 30, and 12 K.

continues to shift to higher frequency as temperature decreases (Figures 12−14). The DOD bending mode absorption in glycerol has the same features as the HOH bending mode: it shifts to higher frequency, broadens, and diminishes (Figure 16).

The absorption from the OH and OD stretching modes for glycerol/water are continuous with change in temperature, as shown in Figures 17 and 18. There is increase in intensity and shift to lower frequency as temperature decreases. The OH stretch region for the glycerol/water glass remains broad over the entire temperatures. The spectral shifts for both bending and stretching modes are consistent with increased H-bonding strength as temperature decreases. The HOH and DOD bending modes and the OH and OD stretching modes show similar temperature dependence, although the overall change in frequency with temperature is larger for HOH than DOD (Figures 19 and 20). For all bands, the widths are also narrower for groups involving deuterium relative to hydrogen (see Table 2).

TABLE 4: Absorption Maxima and Widths of CH Stretching and Bending Modes of Glycerol[a]

	temp, K	C−H bend	C−D bend	C−H stretch (sym)	C−H stretch (asym)	C−D stretch (sym)
glycerol	295			2883 (38)	2935 (43)	
	12			2878 (47)	2932 (45)	
glycerol/D_2O (6/4)	295	1460 (32)		2885 (31)	2940 (49)	
	12	1458 (37)		2883 (29)	2937 (42)	
D_3-glycerol	295	1460 (22)		2880 (30)	2933 (51)	
	12	1458 (22)		2879 (30)	2932 (44)	
D_3-glycerol/D_2O (6/4)	295	1460 (20)		2885 (31)	2940 (49)	
	12	1458 (18)		2883 (29)	2937 (42)	
D_8-glycerol	295		1204 (23)			2105 (39)
	12		1208 (26)			2104 (35)
D_8-glycerol/H_2O (6/4)	295					2108 (30)
	12					2107 (36)

[a] Pk-Center, cm^{-1}, of the peak with a Voigt fit. In parentheses: fwhm, cm^{-1}.

Glycerol/water solvent is widely used to study proteins. Two aspects of the solvent, its dipolar nature and its viscosity, directly play a role in stabilizing proteins. Many protein motions are dependent upon solvent motions, and therefore solvent motions, as indicated by viscosity, affect protein function.[31,32] Many experiments of biological material show evidence of coupling of motion of solvent and protein. The highest resolution spectroscopy is optical hole burning, where spectral line changes occur at the lowest temperature consistent with low energy barriers.[33−35] Fluorescence line narrowing is another site selection technique, and loss of resolution for a chromophore in a protein at around 30 K indicates fluctuations at low temperature.[36] We note that in this temperature range, the IR spectrum of the solvent water molecule is also changing. The highly polar nature of water is critical since changes in the position of water will affect the dipoles of neighboring groups. Such a mechanism was invoked for the low-temperature spectral changes in horseradish peroxidase.[37] The protein may have motions that are not dependent upon the viscosity of the medium; in cytochrome *c*, a major source of optical spectral broadening arises from motion that is not solvent viscosity dependent[38] but could be dependent upon changing bonding networks of water.

In our IR experiments, we cannot tell how fast the solvent can rearrange at a given temperature. On the time scale of our experiments, hours, the sample appeared stable. This point will be investigated later, but other experiments indicate a wide range of relaxation times. Prokratov et al. studied spectral diffusion dynamics of a heme protein in glycerol/water glass and in dry sugar film.[39] The diffusion was faster in the water-containing matrix, and the dynamics occurred over a wide time scale, including hours and days. Water is highly polar, and another spectroscopic means to monitor relaxation times of water is by fluorescence spectral shifts. Properties of tryptophan and indole absorption and emission changed over the 295 to 12 K temperature range, and spectral shifts were attributed to solvent rearrangement.[40] When the solvent cannot rearrange, such as in a water-free glassy sugar matrix, spectral shifts of tryptophan were not seen or greatly reduced.[41] Changing H-bonding even at low temperature will have effects on protein reactions. For instance, the motion of the water in the solvent is evoked to explain features of kinetics of the internal binding of CO in myoglobin.[31,42]

The C−H stretching modes of glycerol are temperature independent (Figure 21). Weak H-bonds between aliphatic and O acceptors (C−H- - -OH_2) have been proposed,[43,44] and they have also been suggested by ab initio calculations.[45] Since the dipole moment of the C−H or C−D bond is very low, H-bonding effects would be expected to be weak, and this is probably why spectral changes are not detectable in the condensed phase that we are studying. The CH_2 and CD_2 bending modes were also identified. Within the experimental resolution, there are also no changes in these bending modes with temperature.

The solution of glycerol/water is not the sum of the individual components. A new absorbance was observed that depends on the isotope of the exchangeable protons of glycerol. This absorbance is seen in Figure 9 at around 1400 cm^{-1} when H_2O is added to perdeuterated glycerol, which would result in deuterated glycerol except for the exchangeable H's of the hydroxyl groups, which would be protonated. An underlying absorbance is also seen in glycerol that is not seen in D_3-glycerol (Figure 8). We suggest that this arises from a bending motion of −COH that is H-bonded to a neighboring glycerol. Interactions between glycerol molecules have also been suggested by dielectric spectroscopy.[46]

In summary, the results presented in this article establish that the glycerol/water solvent H-bonding changes over the temperature range of 295−12 K, a finding that is relevant to many spectroscopic studies and to studies of molecular dynamics.

Acknowledgment. We thank Dr. Nebojsa Marinkovic of the Brookhaven National Laboratory for help in preliminary experiments and useful discussions. We thank Mr. Wayne Wright for help with some experiments and Ms. Jennifer Dashnau for constructive suggestions. The National Institute of Health Grant PO1 GM 48130 supported this work.

References and Notes

(1) Douzou, P. *Cryobiochemistry. An Introduction*; Academic Press: London, 1977.
(2) Sousa, R. *Acta Crystallogr.* **1995**, *D51*, 271.
(3) Allerhand, A.; von Rague Schleyer, P. *J. Am. Chem. Soc.* **1962**, *85*, 1715.
(4) Jeffrey, G. A. *An Introduction to Hydrogen Bonding*; Oxford University Press: New York, 1997.
(5) Pimental, G. C.; McClellan, A. L. *The Hydrogen Bond*; Freeman: San Francisco, California, 1960.
(6) Kaposi, A. D.; Fidy, J.; Manas, E. S.; Vanderkooi, J. M.; Wright, W. W. *Biochim. Biophys. Acta* **1999**, *1435*, 41.
(7) Manas, E. S.; Getahun, Z.; Wright, W. W.; DeGrado, W. F.; Vanderkooi, J. M. *J. Am. Chem. Soc.* **2000**, *122*, 9883.
(8) Walsh, S. T. R.; Cheng, R. P.; Daggett, V.; Vanderkooi, J. M.; DeGrado, W. F. *Protein Sci.* **2003**, *12*, 520.
(9) Herzberg, G. *Infrared and Raman Spectra of Polyatomic Molecules*; Van Nostrand: New York, 1945.
(10) Bertie, J. E.; Ahmed, M. K.; Eysel, H. H. *J. Phys. Chem.* **1989**, *93*, 2210.
(11) Diem, M. *Introduction to Modern Vibrational Spectroscopy*; John Wiley & Sons: New York, 1993.
(12) Devlin, J. P.; Sadlej, J.; Buch, V. *J. Phys. Chem. A* **2001**, *105*, 974.
(13) Marechal, Y. *J. Phys. Chem.* **1993**, *97*, 2846.
(14) Venyaminov, S. Y.; Prendergast, F. G. *Anal. Biochem.* **1997**, *248*, 234.
(15) Wyss, H. R.; Falk, M. *Can. J. Chem.* **1970**, *48*, 607.
(16) Sukarova, B. M.; Sherman, W. F.; Wilkinson, G. R. *Spectrochim. Acta* **1985**, *41*, 315.
(17) Whalleny, E.; Bertie, J. E. *J. Chem. Phys.* **1967**, *46*, 1271.
(18) Bratos, S.; Ratajczak, H.; Viot, P. Properties of H-Bonding in the Infrared Spectral Range. In *Hydrogen-Bonded Liquids*; Dore, J. C., Teixeira, J., Eds.; Kluwer Academic Publishers: Dordrecht, The Netherlands, 1991; p 221.
(19) Ramos, M. A.; Talon, C.; Jimenez-Rioboo, R. J.; Vieira, S. *J. Phys.: Condens. Matter* **2003**, *15*, S1007.
(20) Martinez, L. M.; Angell, C. A. *Nature (London)* **2001**, *410*, 663.
(21) Angell, C. A. *Chem. Rev.* **2002**, *102*, 2627.
(22) Uchino, T.; Yoko, T. *Science* **1996**, *273*, 480.
(23) Challi, R.; Procacci, P.; Cardini, G.; Califano, S. *Phys. Chem. Chem. Phys.* **1999**, *1*, 879.
(24) Perova, T. S.; Christensen, D. H.; Rasmussen, U.; Vij, J. K.; Nielsen, O. F. *Vib. Spectrosc.* **1998**, *18*, 149.
(25) Lunkenheimer, P.; Schneider, U.; Brand, R.; Loidl, A. *Contemp. Phys.* **2000**, *41*, 15.
(26) Wiedersich, J.; Surovtsev, N.; Rossler, E. *J. Chem. Phys.* **2000**, *113*, 1143.
(27) Pauling, L. *J. Am. Chem. Soc.* **1935**, *57*, 2680.
(28) DiMarzio, E. A.; Stillinger, F. H., Jr. *J. Chem. Phys.* **1964**, *40*, 1577.
(29) Tajima, Y.; Matsuo, T.; Suga, H. *Nature (London)* **1982**, *299*, 810.
(30) Hernandez, J.; Uras, N.; Devlin, J. P. *J. Chem. Phys.* **1998**, *108*, 4525.
(31) Frauenfelder, H.; Fenimore, P. W.; McMahon, B. H. *Biophys. Chem.* **2002**, *98*, 35.
(32) Fenimore, P. W.; Frauenfelder, H.; McMahon, B. H.; Parak, F. *Proc. Natl. Acad. Sci. U.S.A.* **2002**, *99*, 16047.
(33) Skinner, J. L.; Friedrich, J.; Schlicter, J. *J. Phys. Chem. A* **1999**, *103*, 2310.
(34) Zollfrank, J.; Friedrich, J.; Vanderkooi, J. M.; Fidy, J. *Biophys. J.* **1991**, *59*, 305.
(35) Fritsch, K.; Eicker, A.; Friedrich, J.; Kharlamov, B. M.; Vanderkooi, J. M. *Europhys. Lett.* **1998**, *41*, 339.

(36) Koloczek, H.; Fidy, J.; Vanderkooi, J. M. *J. Chem. Phys.* **1987**, *87*, 4388.
(37) Zelent, B.; Kaposi, A. D.; Nucci, N. V.; Sharp, K. A.; Dalosto, S. D.; Wright, W. W.; Vanderkooi, J. M. *J. Phys. Chem. B* **2004**, *108*, 10317.
(38) Prabhu, N. V.; Dalosto, S. D.; Sharp, K. A.; Wright, W. W.; Vanderkooi, J. M. *J. Phys. Chem. B* **2002**, *106*, 5561.
(39) Ponkratov, V. V.; Friedrich, J.; Vanderkooi, J. M. *J. Chem. Phys.* **2002**, *117*, 4594.
(40) Dashnau, J. L.; Zelent, B.; Vanderkooi, J. M. *Biophys. Chem.*, in press.
(41) Wright, W. W.; Guffanti, G.; Vanderkooi, J. M. *Biophys. J.* **2003**, *85*, 1980.
(42) Frauenfelder, H.; McMahon, B. H.; Austin, R. H.; Chu, K.; Groves, J. T. *Proc. Natl. Acad. Sci. U.S.A.* **2001**, *98*, 2370.
(43) Sutor, D. J. *Nature* **1962**, *195*, 68.
(44) Gu, Y.; Kar, T.; Scheiner, S. *J. Am. Chem. Soc.* **1999**, *121*, 9411.
(45) Pohle, W.; Gauger, D. R.; Bohl, M.; Mrazkova, E.; Hobza, P. *Biopolymers* **2004**, *74*, 27.
(46) Lunkenheimer, P.; Pimenov, A.; Dressel, M.; Goncharov, Y. G.; Bohmer, R.; Loidl, A. *Phys. Rev. Lett.* **1996**, *77*, 318.